Characterization of Colored Dissolved Organic Matter Using High-Energy Laser Fragmentation

ARTICLE *in* ENVIRONMENTAL SCIENCE AND TECHNOLOGY · JUNE 2000

Impact Factor: 5.33 · DOI: 10.1021/es9911263

2 AUTHORS, INCLUDING:

P. G. Coble
University of South Florida
79 PUBLICATIONS **3,882** CITATIONS

Environ. Sci. Technol. **2000**, *34,* 3283−3290

Characterization of Colored Dissolved Organic Matter Using High-Energy Laser Fragmentation

JENNIFER R. BOEHME* AND PAULA G. COBLE

Department of Marine Science, University of South Florida, 140 7th Avenue South, St. Petersburg, Florida 33701

A new approach combining high-energy laser fragmentation (HELF) with excitation−emission matrix spectroscopy (EEMS) was used to study colored dissolved organic material (CDOM) in rivers feeding the Tampa Bay Estuary. Results presented as difference spectra showed that fluorescent material destroyed had two distinct peaks for all samples at all degradation wavelengths of 320 nm or greater. All samples showed highest loss of UV−C (220−280 nm) stimulated fluorescence, even when irradiated at 390 nm, with lower loss of UV−B (280−320 nm) stimulated fluorescence centered around the wavelength used for degradation. In contrast to spectra for the initial and residual fingerprints, loss spectra showed the rounded contours expected for a pure organic fluorophore. These observations suggest that laser irradiation targets a specific fluorophore or restricted group of fluorophores in the original mixture, some of which have a double excitation maximum and single emission maximum. By varying the degradation wavelength, eight distinct fluorophore groups were identified in the sample set, some of which were unique to either river or estuarine samples and some of which were common to samples from both environments.

Introduction

Interaction of light with naturally occurring colored dissolved organic material (CDOM) has important consequences for studies of environmental biology and chemistry. Photophysical processes, in which absorption of light energy does not result in a chemical reaction, have applications to the study of ocean color, differentiation of pollutants in water samples, discrimination of CDOM from different sources, and calculation of solar irradiance available for photosynthesis. Photochemical processes, in which the CDOM is destroyed or stimulates secondary reactions, play an important role in cycling of carbon, trace elements, and pollutants in natural waters. Improved knowledge of the chemical structures of the chromophores that comprise CDOM is therefore essential for advancing the understanding of these related processes in both freshwater and marine environments.

Defined on the basis of absorbance of UV and visible light, CDOM includes the chromophoric (light absorbing) and fluorophoric (light emitting) components of aquatic humic substance. Absorption spectra for both CDOM and aquatic humic substance show exponential increase with decreasing wavelength, presumably arising from the presence of a wide variety of individual chromophores with overlapping absorption maxima. CDOM fluorophores also show excitation and emission properties similar to those of isolated humic substances from soils, rivers, and the open ocean (*1*−*3*). However, the excitation spectrum of CDOM does not correspond to the absorbance spectrum, indicating that not all CDOM fluoresces.

Chromophoric and fluorophoric species provide sites within CDOM for light stimulated reactions; thus spectral properties of CDOM provide a window into the photoreactive portion of the chemical structure. Although several identifiable fluorophores have been isolated from water samples, none are present in sufficient quantities to account for DOM fluorescence. Thermochemolysis of Suwanee River DOM has been shown to release benzene-, phenol-, and toluene-containing compounds (*4*), which are potential fluorophores derived from the oxidation of lignin and cutan. Fulvic acids and humic acids isolated from the same soil or water sample have slightly different excitation and emission maxima, with a red shift for both properties in the humic fraction. This is consistent with other chemical assays, which show more extensive conjugation, higher molecular weight, and increased aromaticity in humic acid relative to fulvic acid. Similar observations of red-shifted maxima in terrestrial and riverine CDOM relative to marine CDOM have an analogous interpretation. Fluorophoric and chromophoric moieties can thus be envisioned as being incorporated within the complex backbone of the macromolecular structure of aquatic humic substance.

Previous photochemical studies have shown overall correspondence between absorption coefficient and the rate of both CDOM degradation (*5*−*7*) and photoproduct formation (*8*−*12*). These observations suggest that there are a limited variety of photoreaction pathways. The action spectra for most processes show a maximum between 300 and 350 nm, corresponding to the UV−B excitation maximum for CDOM. Studies of reaction mechanisms have focused more on the destruction of organic pollutants and the production of reactive intermediates, such as singlet oxygen and peroxide, than on consequences to the aquatic humic molecular structure.

Since identifiable photoproducts are not colored and CDOM is not identifiable in its native state, not much is known about specific structural changes to fluorophores induced by sunlight. Studies using monochromatic irradiation from xenon or mercury lamps (*7, 13, 14*) have shown that maximum bleaching (loss of color) and loss of fluorescence occurs at or near the wavelength used for degradation (λ_{deg}). New fluorescence production, photoreversibility, and dark regeneration of fluorescence has been reported for some water samples (*14, 15*).

The purpose of this study was to investigate wavelength-dependent effects of light on CDOM from coastal environments. Samples from four rivers entering Tampa Bay and from the estuary itself were examined using excitation−emission matrix spectroscopy (EEMS) before and after exposure to a Class IV laser. Results show that exposure to high-energy monochromatic light provides new insight into the composition of CDOM. New information on the photophysical properties of several subsets of CDOM fluorophores is presented.

Experimental Methods

Samples were obtained from eight sites in the four major rivers entering Tampa Bay. These sites had been shown to be representative of both salinity gradients in the estuary

* Corresponding author phone: (727)553-1130; fax: (727)553-1189; e-mail: jboehme@marine.usf.edu.

10.1021/es9911263 CCC: $19.00
Published on Web 06/23/2000

and of relative importance of each river to total freshwater supply in the bay. Number of samples and respective salinities were as follows: Hillsborough River ($n = 1$; $S = 0$), Alafia River ($n = 1$; $S = 7.5$), Little Manatee River ($n = 2$; $S = 0, 20.5$), and Manatee River ($n = 4$; $S = 0, 2.5, 19, 23$).

Samples were collected in amber glass bottles just below the water's surface, placed on ice until processing (less than 3 h), and filtered using 0.45-μm nylon filters. The filters were prerinsed with methanol and water to remove potential fluorescent contamination. CDOM samples were refrigerated until analysis (less than 2 weeks). Salinities were determined using a refractometer with automatic temperature correction (Leica). Absorption from 750 to 220 nm was measured in a 1-cm quartz cell against a MilliQ water blank using a Hitachi U-3300 double beam absorption spectrophotometer. Samples were diluted with MilliQ water so the optical density at 300 nm was <0.02 (*3*).

Excitation emission matrixes (EEMs) were generated with a Fluoromax-2 spectrofluorometer (Instruments SA Inc., Edison, NJ) covering an excitation range of 220−455 nm and an emission range of 250−600 nm. The Fluoromax-2 is equipped with a 150-W xenon arc lamp, a temperature-controlled cuvette holder (set to 19 °C for all analyses), and an air-cooled, red-sensitive PMT. The instrument configuration included a single excitation monochromator (1200 grooves/mm) blazed at 250 nm and a single emission monochromator (1200 grooves/mm) blazed at 500 nm. Samples were placed in 1-cm quartz cells and analyzed in ratio mode with a 5-nm bandwidth for both excitation and emission. Excitation correction factors were generated from 220 to 455 nm by placing a solution of 8 g/L Rhodamine B (laser grade quality in ethylene glycol) in the sample cuvette and collecting an excitation spectrum was from 200 to 600 nm with emission set to 630 nm. The spectrum was inverted and normalized to produce correction factors. Emission correction factors from 250 to 600 nm were generated using a standard lamp assembly (200-W quartz-halogen tungsten-coiled filament lamp) operated at 6.0 amp at a distance of 50 cm. Values obtained were then divided into the known irradiance values of the lamp at each wavelength and normalized to produce correction factors. Fluorescence was corrected for instrument and lamp variability and normalized to quinine sulfate fluorescence as described previously (*16*, method 1).

It has been reported that fluorescence intensity of CDOM varies with pH (*17*−*19*). The effects of pH on filtered water were tested using a river station and a coastal station at the pH range found within the estuary. The pH range of filtered water samples from the study was surprisingly narrow, between 7 and 8.5. Water samples were run at pH 7.0, 8.5, and at the sample's unaltered pH. The emission wavelengths used for the analysis were from 430 to 470 nm at excitations 245 and 350 nm. The excitation wavelengths were chosen because the first is close to the UV−C excitation maximum and the second wavelength has been used in previous studies. Results indicated that for this range of pH the percent coefficient of variability around the mean was less than 5% for all stations at both excitation wavelengths, indicating that in this pH range the fluorescence intensities do not change appreciably.

Photodegradation experiments were conducted in the dark. Degradation wavelengths (λ_{deg}) were generated by pumping an optical parametric oscillator (OPO) with the third harmonic output of a Nd:YAG laser (355 nm) pulsed at 10 Hz (both by Spectra-Physics Lasers, Terra Bella, CA). The OPO included a frequency doubler, enabling a tuning range of 220 nm−2 μm (*20*). The frequency doubler output was focused to 6 mm diameter using a pair of lenses ($F = 100$ and −50). Power output was recorded by diverting a small amount of the beam to a photodiode power meter (Ophir Optronics). At 280, 305, and 390 nm, the average output and exposure times were 0.220 mJ/pulse for 4 min. Average output at 320 and 340 nm was 0.125 mJ/pulse, and exposures were 8 min. Samples were placed in a 1-cm quartz cuvette in the beam path and stirred continuously to ensure exposure of the entire sample volume. No noticeable differences in temperature were observed after sample exposure. After exposure, the sample cuvette was immediately transferred to the spectrofluorometer, and its fluorescence matrix was generated and corrected. The absorbance spectrum of the degraded sample was then collected. The corrected fluorescence matrix for each degraded sample (EEM_d) was subtracted from that of the undegraded starting material (EEM_u) to generate a fluorescence loss spectrum ($EEM_{loss} = EEM_u - EEM_d$). Results are presented as loss spectra.

Statistics used to determine peak variability included a test for normal distribution of the data set, a test for equal variance of the data set, and a one-way Anova (95% confidence level) coupled with a Tukey test to determine variability at individual wavelengths. For data where the variance test failed, a Mann−Whitney rank sum analysis was performed to determine variability.

Results and Discussion

Figure 1 shows a typical EEM before degradation (EEM_u). Initial fluorescence properties of all samples were nearly identical, despite a range in salinity of 0−23, and the undegraded EEM in Figure 1 is typical of CDOM from other coastal areas (*2*, *21*, *22*). The two fluorescence peaks are designated A and C according to previously published nomenclature (*22*). The fluorescence intensity of peak A was more intense than peak C, with an excitation maximum (ex_{max}) at 235 nm. The ex_{max} for peak C was at 310−315 nm. Although the emission maxima (em_{max}) for both peaks occurred between 440 and 445 nm in these samples, an offset is often observed in natural CDOM samples (*1*−*3*). Average positions of fluorescence maxima (ex_{max}/em_{max}) and the ratio of fluorescence intensity of peaks A and C are listed in Table 1 for the entire sample set, which has been divided into riverine and estuarine categories based on the salinity range (S) of samples assigned to each group.

Unlike the rounded contours expected for a pure organic fluorophore such as quinine sulfate (Figure 1), peak C has a trailing edge with increasing em_{max} as excitation wavelength increases, resulting in diagonal elongation of the peak (line X; Figure 1). This type of peak elongation is a feature of natural CDOM and is attributed to the presence of multiple fluorophores, intermolecular energy transfer, or both conditions (*2*, *21*−*24*). Although it has been suggested that some fluorophores in this pool display both peak A and C fluorescence (*21*, *22*), the offset in em_{max} and variability in the ratio of fluorescence intensity of the two peaks (A:C) indicates that compounds with A-only or C-only fluorophores are also present. The term fluorophore is used in its most general sense, as the structure from which fluorescence arises. Given the complexity of CDOM, this includes individual chemical molecules suspended in solution as well as individual moieties or multiple, associated moieties which are incorporated into larger nonfluorescent molecular structures and contribute to total fluorescence signal.

A typical EEM for a degraded sample (EEM_d) is also shown in Figure 1. Despite overall similarity in EEMs before and after exposure, closer inspection of EEM_d data revealed small shifts in position of ex_{max}/em_{max} toward both shorter and longer wavelengths, depending on the wavelength of degradation relative to the position of the original ex_{max}/em_{max}. Our results, which agreed with previous observations (*14*, *15*), showed red shifts in em_{max} for samples exposed to radiation at 320 nm and lower and blue shifts for exposure to radiation above 320 nm.

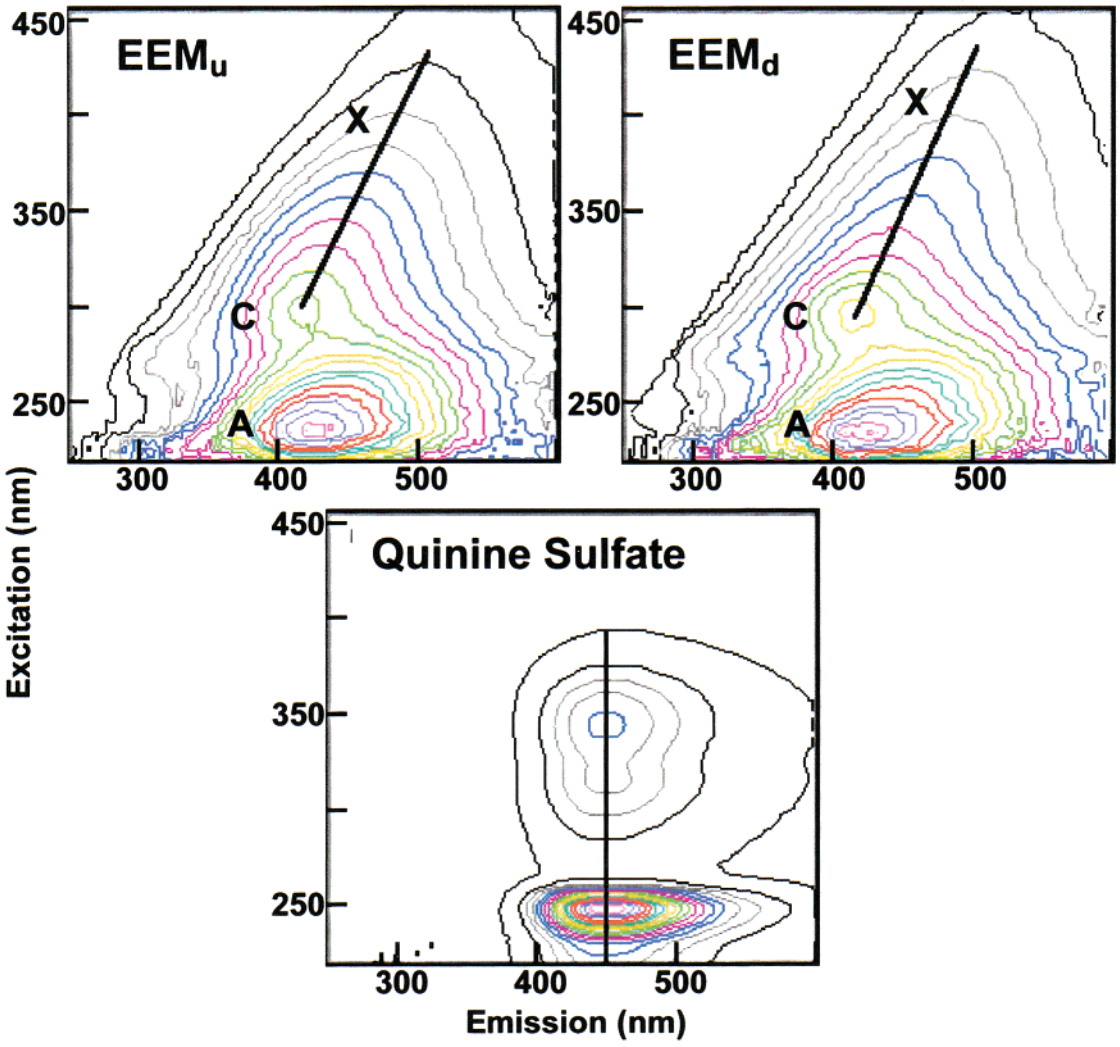

FIGURE 1. Contour plots for an Alafia River sample before (EEM_u, upper left panel) and after (EEM_d, upper right panel) exposure to 340 nm light and for quinine sulfate (bottom panel). Each contour represents 5% of the total intensity. Total concentrations for each sample were as follows: EEM_u, 15.4 quinine sulfate equivalents (QSE); EEM_d, 10.8 QSE; quinine sulfate, 447 QSE.

Absorption spectra run before and after degradation showed negligible differences at all λ_{deg} except for a slight peak near 280 nm in the samples degraded at this wavelength. Lack of significant changes was most likely the result of experimental procedures, in which samples were diluted to prevent inner filter effects in fluorescence analyses and exposures where performed on small volumes (<2 mL) in 1-cm cuvettes. These volumes and concentrations were adequate for the more sensitive fluorescence assays; however, they were not optimal for collection of reliable absorbance difference spectra.

The main features of all EEM_{loss} generated by degradation wavelengths of 320 nm or greater are shown in Figure 2. Fluorescence loss was observed as two peaks with identical emission maxima and circular contours, similar to the EEM of pure quinine sulfate. Each λ_{deg} caused loss of a slightly different pool of fluorophores, with a shift in peak positions for both A and C toward longer wavelengths as λ_{deg} increased (Figure 2). There was also a trend toward longer wavelength em_{max} with decreasing salinity within each river basin (Table 1). At λ_{deg} 320 and 340, loss peaks for riverine and estuarine samples were statistically different, indicating the presence of fluorophores unique to rivers but absent or reduced in the estuary and vice versa. Loss peaks from λ_{deg} 390 were considerably red-shifted in both excitation and emission maxima and were statistically different from peaks produced at the other degradation wavelengths; however, riverine and estuarine samples were not different.

The rounded contours of loss peaks suggest that a small pool of fluorophores was selectively destroyed at each specific λ_{deg}. Disappearance of the A peak from irradiation at the absorbance maximum for peak C further indicates that a significant fraction of the fluorophores removed had dual excitation maxima since it is unlikely that much radiation at 320 nm and higher would be absorbed by a compound with a single absorbance maximum at 250 nm. This evidence of direct coupling of peaks A and C in a single fluorophore is strengthened by the observation that A and C have the same em_{max} in EEM_{loss} from each λ_{deg}. It seems unlikely that the photochemical coupling between A and C is due to intermolecular energy transfer since the emission of the A peak does not overlap closely with the excitation of the C peak, a necessary prerequisite for efficient intermolecular transfer (*26*).

In contrast to previous reports of maximum loss of fluorescence at or near λ_{deg} (*14*), these results show that the highest fluorescence loss occurred for peak A at 240−260 nm. Ratios of A:C were always greater than 1 and decreased with increasing λ_{deg} (Table 1). The relative loss in fluorescence intensity following irradiation decreased for peak A from 28% at 320 nm to 15% at 390 nm. For peak C, losses ranged from 25 to 36%, with no observed trend with λ_{deg}. There are several

TABLE 1. Average Excitation/Emission Maxima (ex_{max}/em_{max}), Percent Loss and Gain, Ratio of Fluorescence Intensity of Peaks A and C (A:C), and Fluorophore Type (peak ID) for Peaks Identified in Loss EEMs

		riverine (*S*, 0−2.5)				estuary (*S*, 7.5−23)			
λ_{deg} loss		ex_{max}/em_{max}[a] (*n* = 4)	loss (%)	A:C[a]	peak ID	ex_{max}/em_{max}[a] (*n* = 4)	loss (%)	A:C[a]	peak ID
undegraded	A	236/446		1.92		236/444		2.1	
	SD	2.2/3.0		0.66		2.5/5.6		0.07	
	C	316/442				310/441			
	SD	6.5/4.4				7.1/3.4			
280	A	255/456	49.7	**2.85**	1	258/451	32.0	**4.29**	1
	SD	5.8/1.9	4.4	0.49		5.8/6.4	3.1	0.98	
	C	351/463	39.8		7	358/469	17.2		7
	SD	8.5/3.7	8.3			7.6/5.8	3.1		
305	A	253/**442**	35.5	1.61	1	247/**433**	40.3	1.8	1
	SD	2.9/4.1	4.7	0.18		12/7.0	4.5	0.19	
	C	301/**447**	37.7		4	297/**432**	41.3		3
	SD	4.8/6.2	4.3			5.8/5.8	9.3		
320	A	253/**449**	28.0	1.66	1	240/**433**	28.6	1.76	1
	SD	2.9/7.8	6.9	0.11		4.1/2.8	3.0	0.05	
	C	330/**449**	32.0		6	311/**429**	32.8		5
	SD	18/4.9	6.6			4.8/4.3	3.6		
340	A	252/**456**	20.1	1.57	1	249/**444**	24.2	1.8	1
	SD	5.0/1.9	8.1	0.16		7.5/9.4	5.0	0.14	
	C	340/**454**	25.4		6	325/**442**	27.4		6
	SD	18/6.2	8.6			0/5.4	5.1		
390	A	260/479	18.3	1.28	2	264/483	14.8	1.28	2
	SD	7.1/5.2	4.8	0.12		2.5/6.3	2.5	0.03	
	C	374/469	35.8		8	377/476	28.0		8
	SD	2.5/4.4	13.0			2.9/3.5	6.0		

		gain (%)			gain (%)		
gain		ex_{max}/em_{max}[a] (*n* = 2)	loss (%)	A:C[a]	ex_{max}/em_{max}[a] (*n* = 2)	loss (%)	A:C[a]
390	A	245/404	11.7	1.55	240/411	15.6	2.25
	SD	0/2.8	0.98	0.01	7.1/1.4	3.7	0.61
	C	323/411	13.1		328/410	17.7	
	SD	3.5/1.4	2.5		3.5/2.8	8.4	

[a] Numbers in bold indicate that significant differences were found between estuarine and riverine data at that degradation wavelength.

possible interpretations for these results. As λ_{deg} increases, the possibility of overlap with absorbance bands of peak A fluorophores is lessened; therefore, decreasing the loss of fluorescence from A-only compounds. The lower A:C ratio may also be partly representative of the intrinsic properties of various A+C fluorophores removed by each λ_{deg}. These results cannot determine the relative importance of these two explanations.

New fluorescence peaks were produced in four of the samples exposed to λ_{deg} 390 (Figure 2) in quantities which represented a 12−18% increase in fluorescence intensity (Table 1). The ex_{max}/em_{max} of these new peaks were shifted toward the blue relative to the loss peaks, with ex_{max} at 242 and 325 nm and em_{max} at 410 nm. The blue shift of the new peak would be consistent with the formation of a fluorescent product with a lower molecular weight through processes such as fragmentation of one component in a multi-ring compound or a photo-Fries rearrangement, although many different types of reactions are possible. While peak production has been previously observed in riverine samples due to exposure to monochromatic light below 320 nm (*14*), we did not observe fluorescence generation at wavelengths other than 390. These peaks were produced in both riverine and estuarine stations.

In contrast to the selective removal of fluorophores observed above 320 nm, loss EEMs for samples degraded at 280 and 305 nm did not show rounded contours (Figure 3). The dominant feature was removal of peak A fluorescence with the broad emission maxima and elongated C peak observed in undegraded CDOM (Figure 1). Although discrete C peaks were difficult to detect in EEM_{loss} from these λ_{deg}, significant losses of fluorescence occurred across a broad range of the matrix. Irradiation at the shorter wavelengths also induced greater total loss of fluorescence intensity for both A and C peaks, despite similar total exposure energy for all λ_{deg}. In riverine samples nearly half of initial A peak fluorescence was destroyed (Table 1). A:C ratios of loss EEMs at 280 nm were significantly higher than in initial samples, with a maximum of 4.3 observed in estuarine samples. Although this is high as compared to the range observed in unaltered natural waters (*22*), it is roughly equivalent to the A:C ratio for quinine sulfate (*27*). The broad band emission and shape of peak C indicates that many compounds were effected and the high A:C is most likely due to predominant loss of A-only fluorophores. Estuarine samples ($S > 7$) displayed a generally broader emission band than the riverine counterparts for both λ_{deg}, possibly due to a higher diversity of fluorophores present in the initial samples.

Overall, results indicate that irradiation at 280 and 305 nm is more destructive than at the longer wavelengths and also targets a wider variety of fluorophores. High A:C ratios and lack of a distinctive loss peak in the C region suggests that much of the material destroyed probably has only a single UV−C excitation maximum. Estuarine samples appear to be enriched in these compounds relative to riverine samples.

To test for significant differences observed between samples from riverine and estuarine environments and to ascertain whether HELF at different λ_{deg} targeted distinctive pools of fluorophores, a Tukey test was applied to ex_{max} and

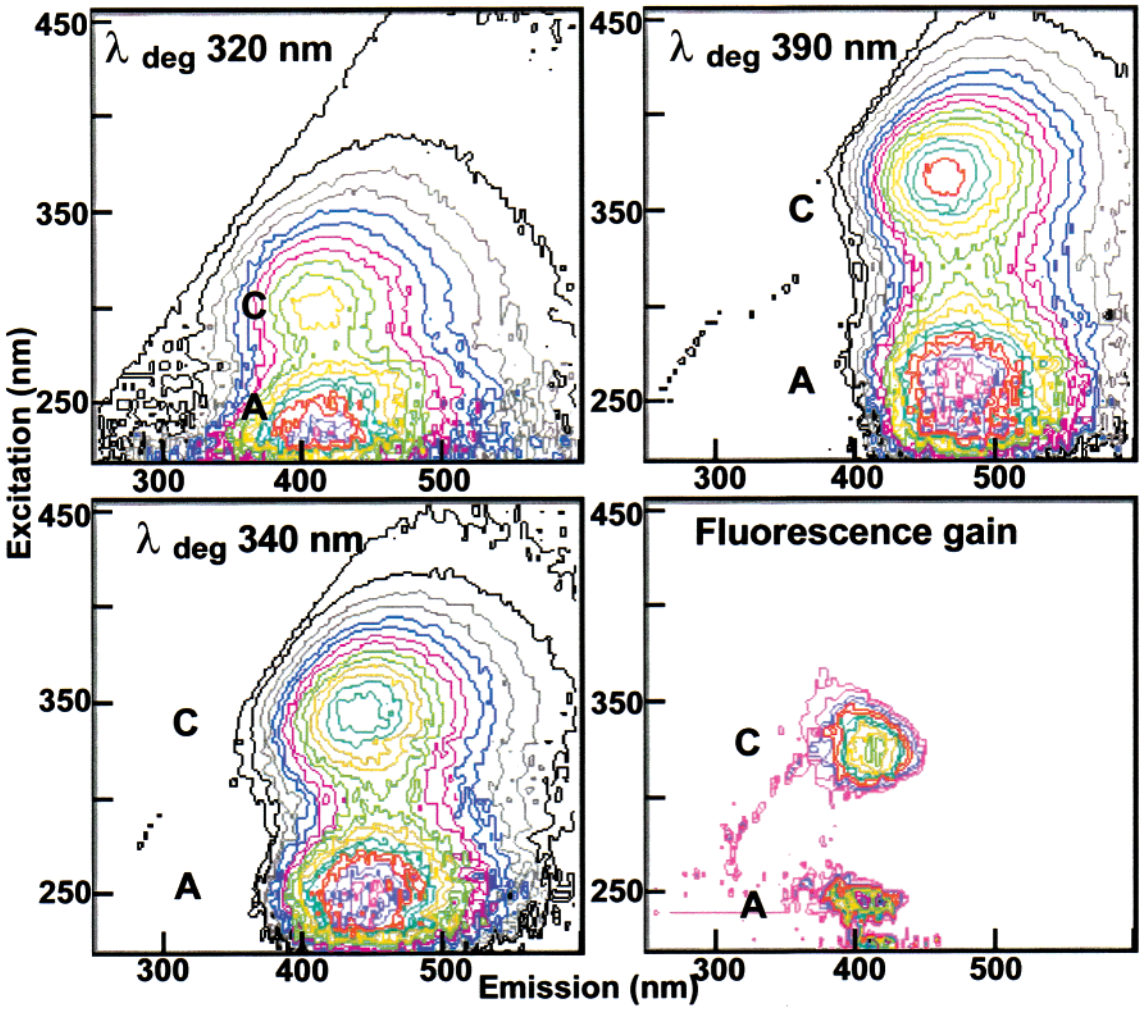

FIGURE 2. EEM_{loss} contour plots of fluorescence loss for λ_{deg} 320 nm (Alafia River, upper left panel), 340 nm (Little Manatee River, lower left panel), and 390 nm (Little Manatee river, upper right panel). EEM_{gain} contour plot for λ_{deg} 390 nm is shown in the lower right panel. Note the red shift in emission maxima (to the right) and excitation maxima (to the top) with increasing λ_{deg}. Contour lines represent 5% of the total intensity. Total concentrations for each sample were as follows: λ_{deg} 320, 4.97 QSE; λ_{deg} 340, 3.91 QSE; λ_{deg} 390, 3.56 QSE; fluorescence gain, 1.79 QSE.

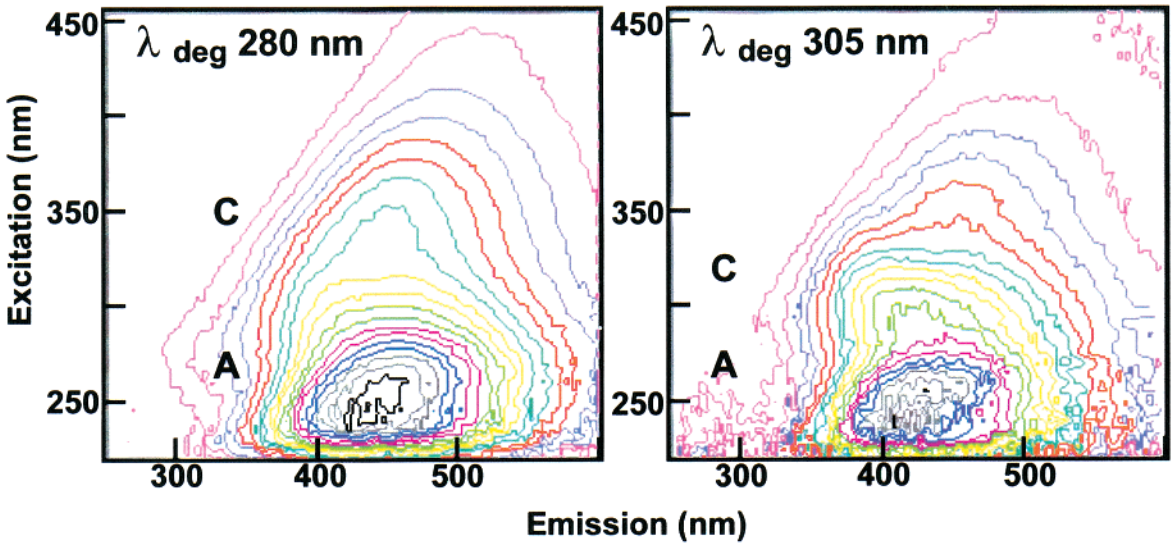

FIGURE 3. Contour plots of fluorescence loss for λ_{deg}: 280 nm (Little Manatee River) and 305 nm (Manatee River). Contour lines represent 5% of the total intensity. Total concentrations for each sample were as follows: λ_{deg} 280, 11.6 QSE; λ_{deg} 305, 6.86 QSE.

em_{max} data for each peak listed in Table 1. For this analysis, A and C peaks were considered separately and not as dual peaks of a single fluorophore. Data printed in boldface in Table 1 indicate significant differences between estuarine and riverine data at a given λ_{deg}. A:C ratios were significantly different only for λ_{deg} 280 nm, whereas em_{max} positions for

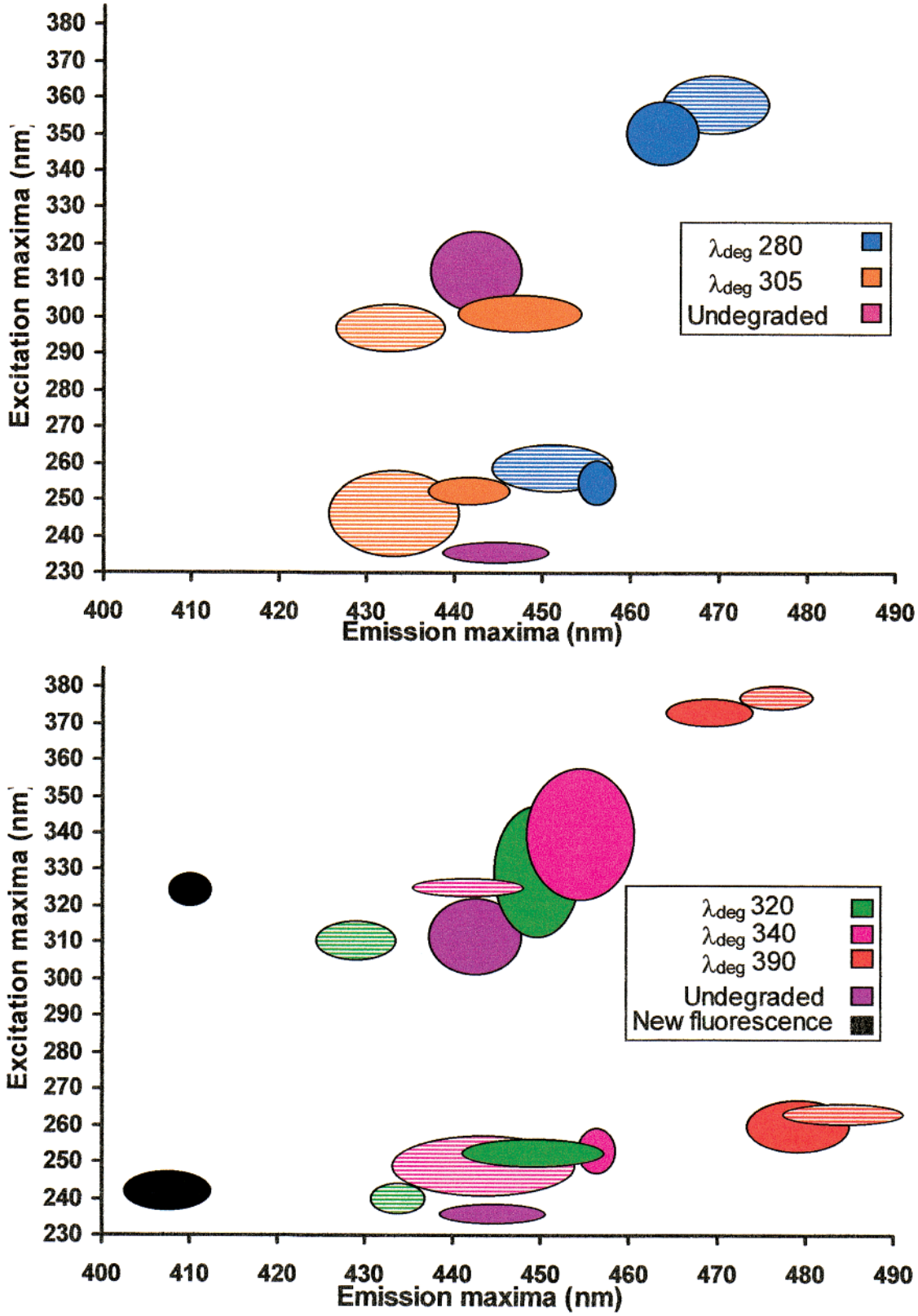

FIGURE 4. Average positions for peaks A and C of EEM_{loss} for all undegraded and degraded riverine (solid bubbles; $S < 2.6$) and estuarine samples (striped bubbles; $S > 7.5$) samples. Height and width of each bubble represent standard deviation of ex_{max} and em_{max}, respectively. Results from $\lambda_{deg} = 320$, 340, and 390 are shown in upper panel; results from $\lambda_{deg} = 280$ and 305 are shown in bottom panel. Numbers refer to peak ID listed in Table 1.

both A and C peaks were significantly different at λ_{deg} 305, 320, and 340. Significant differences in λ_{deg} dependence were also observed. A total of eight unique fluorophores were identified at the 95% confidence level. Low variability in ex_{max} and high standard deviations in em_{max} for A peaks resulted in several of them being classified as fluorophore 1. These results are indicated with fluorophore type numbers in Table 1. A total of eight A peaks were classified as fluorophore type 1, and the remaining two A peaks were identified as type 2. The C peaks separated into six fluorophore types.

All peaks listed in Table 1 are plotted in Figure 4. The center of each bubble represents the position of average ex_{max}/em_{max} for each A and each C peak. Height and width of bubbles represent standard deviation in ex_{max} and em_{max}, respectively. Several general observations are as follows: (i) loss peaks are distributed on both sides of initial peaks in the undegraded sample; (ii) at a given λ_{deg}, estuarine peaks (striped bubbles) fall at shorter wavelengths than do riverine peaks (solid bubbles), (iii) both ex_{max} and em_{max} shift toward longer wavelengths as λ_{deg} is increased, and (iv) the A peak always occurs at $ex_{max} < 270$ nm, even when 280 is used as the λ_{deg}. This last observation emphasizes that the loss EEMs reflect the photophysical properties of the fluorophores destroyed rather than those of all compounds removed or altered by the irradiation.

The fact that material from estuarine sources consistently exhibits significant blue-shifted loss relative to its riverine counterpart has important implications for CDOM chemical composition. Observed changes in the spectral properties of bulk CDOM in riverine and coastal areas have previously been attributed to the effects of environmental factors such as pH (*19*), to production of new fluorescent materials, and to effects of mixing and photodegradation (*25*, *28*). These data show that differences in fluorescence maxima are in part due to presence or absence of discrete fluorophores, which are unique to either marine or terrestrial CDOM, and these compositional changes can occur well inside the mouth of the river at salinities less than 20. The extent of structural differences required to explain fluorescence differences between estuarine and riverine fluorophores pools, i.e., whether it represents a photochemical transformation de novo synthesis, cannot be determined from these data.

Figure 4 also clearly illustrates the complexity of results of this study. Nearly all of the eight unique fluorophore types identified by statistical analysis are most certainly a mixture of compounds, some may have the same fluorophore structure, some may have multiple fluorophores, and some may have a single fluorophore that exhibits multiple fluorescence maxima. The tight coupling between A and C peaks for some λ_{deg} suggests that an A+C fluorophore is a major component in many samples, for example, estuarine samples degraded with 305, 320, and 340 nm light. Strong decoupling between peaks produced in both riverine and estuarine samples at λ_{deg} 280 provides evidence for a large component of A-only compounds.

It should also be noted that due to the short duration of our studies, we are unable to conclude with certainty that fluorophores absent following irradiation were permanently destroyed. Any reaction which disrupts the π^* cloud could result in loss of fluorescence; however, not all of these reactions would also result in permanent damage to the fluorophore. Previous reports of regeneration of fluorescence (*14*, *15*) suggest that these reversible reactions do occur in samples from some environments, but no reaction mechanisms have been demonstrated.

The $EEMs_{loss}$ from many of the individual samples suggest that under some conditions the fluorophores lost are a rather simple mixture of closely related compounds and that environmental variability appears to be responsible for high standard deviation in peak positions. This was a surprising result given the similarity in undegraded EEMs for this limited set of samples. Additional analyses on replicate samples would improve statistical significance of peak separations. However, these results highlight the utility of the HELF technique for elucidation of the photophysical properties of CDOM fluorophores.

The most surprising result, and the one which is most difficult to explain, is that HELF at longer λ_{deg} appears to target specific fluorophores, despite the broad band of absorption maxima for most organic compounds. All of these λ_{deg} are close to the C peak, where fewer compounds are capable of absorption than at 250 nm. One possible explanation is that although bulk CDOM is composed of multiple discrete fluorophores, composition may be dominated by a few major fluorophore structures. Presumably, all compounds capable of absorbing the narrow band λ_{deg} are effected during the irradiations. Many are lost; however, only a few of these are fluorescent, and many may have the same fluorophore. At the shorter λ_{deg} many more compounds are effected, and $EEMs_{loss}$ more closely resemble the complex mixture of bulk CDOM. This study provides important new preliminary data for photophysical properties of subset of CDOM.

Overall results lead to the conclusion that there are more compounds in CDOM with A-only fluorophores than with A+C or C-only fluorophores. This helps to explain the variability in A:C ratios in the environment as well as alterations of fluorescence spectra caused by prolonged exposure to sunlight. CDOM composition and fluorescence has previously been shown to be source dependent, and these results confirm that chemical differences between source material influence the fluorescence variability between riverine and marine endmembers. One important ramification of these results is that exposure of CDOM to sunlight at wavelengths greater than 300 nm will result in significant, simultaneous loss of absorbance at shorter wavelengths. This has important consequences on harmful effects of UV−C radiation on organisms.

Acknowledgments

We thank Dr. Robert Byrne and Dr. Carlos del Castillo for reviews and editorial comments. This research was funded by ONR Contract N00014-96-1-5010 to P.G.C.

Literature Cited

(1) Goldberg, M. C.; Weiner, E. R. *Humic substances in the Suwannee River, Georgia*; U.S. Geological Survey Open-File Report 87-557; U.S. Department of Interior: Washington, DC, 1989; pp 179−204.
(2) Coble, P. G.; Green, S. A.; Blough, N. V.; Gagosian, R. B. *Nature* **1990**, *348*, 432−435.
(3) Green, S. A.; Blough, N. V. *Limnol. Oceanogr.* **1994**, *39*, 1903−1916.
(4) Del Rio, J. C.; Hatcher, P. G. In *Humic and Fulvic Acids*; Gaffney, J. S., Marley, N. A., Clark, S. B., Eds.; American Chemical Society: Washington, DC, 1996; pp 78−95.
(5) Cherrier, J.; Bauer, J.; Druffel, E. R. M.; Coffin, R. B.; Chanton, J. P. *Limnol. Oceanogr.* **1999**, *44*, 730−736.
(6) Kouassi, A. M.; Zika, R. G.; Plane, J. M. C. *Neth. J. Sea Res.* **1990**, *27*, 33−41.
(7) Kieber, R. J.; Zhou, X. L.; Mopper, K. *Limnol. Oceanogr.* **1990**, *35*, 1503−1515.
(8) Kieber, D. J.; McDaniel, J. A.; Mopper, K. *Nature* **1989**, *341*, 637−639.
(9) Mopper, K.; et al. *Nature* **1991**, *353*, 60−62.
(10) Wetzel, R. G.; Hatcher, P. G.; Bianchi, T. S. *Limnol. Oceanogr.* **1995**, *40*, 1369−1380.
(11) Miller, W. L.; Zepp R. G. *Geophys. Res. Lett.* **1995**, *22*, 417−420.
(12) Moran, M. A.; Zepp, R. *Limnol. Oceanogr.* **1997**, *42*, 1307−1316.
(13) Kouassi, A. M.; Zika, R. G. *Toxicol. Environ. Chem.* **1992**, *35*, 195−211.
(14) Ward, K. A. Masters Thesis, Kent State University, 1996.
(15) Kouassi, A. M.; Zika, R. G. *Neth. J. Sea Res.* **1990**, *27*, 25−32.
(16) Coble, P. G.; Mopper, K.; Schultz, C. S. *Mar. Chem.* **1993**, *41*, 173−178.
(17) Laane, R. W. P. M. *Mar. Chem.* **1982**, *11*, 395−401.
(18) Ferrari, G. M. *Remote Sens. Environ.* **1991**, *37*, 89−100.
(19) Pullin, M. J.; Cabaniss, S. E. *Limnol. Oceanogr.* **1997**, *42*, 1766−1773.
(20) Bengtsson, M.; Nilsson, L.-G. Masters Thesis, Lund University, 1996.
(21) De Souza Sierra, M. M.; Donard, O. F. X.; Lamotte, M.; Belin, C.; Ewald, M. *Mar. Chem.* **1994**, *47*, 127−144.
(22) Coble, P. G. *Mar. Chem.* **1996**, *51*, 325−346.

(23) Donard, O. F. X.; Lamotte, M.; Belin, C.; Ewald, M. *Mar. Chem.* **1989**, *27*, 117−136.
(24) Coble, P. G.; Del Castillo, C. E.; Avril, B. *Deep-Sea Res.* **1998**, *45*, 2195−2223.
(25) De Souza Sierra, M. M.; Donard, O. F. X.; Lamotte, M. *Mar. Chem.* **1997**, *58*, 51−58.
(26) Sharma, A.; Schulman, S. G. *Introduction to Fluorescence Spectroscopy*; John Wiley and Sons: New York, 1999.
(27) Velapoldi, R. A.; Mielenz, K. D. *Standard reference materials: A fluorescence standard reference material- quinine sulfate dihydrate*; National Bureau of Standards SP 260-64; U.S. Government Printing Office: Washington, DC, 1980.
(28) Del Castillo, C. E.; Coble, P. G.; Morell, J. M.; López, J. M.; Corredor, J. E. *Mar. Chem.* **1999**, *66*, 35−51.

Received for review October 1, 1999. Revised manuscript received May 9, 2000. Accepted May 11, 2000.

ES9911263